Marine Pollution Bulletin 218 (2025) 118226

Contents lists available at ScienceDirect

Marine Pollution Bulletin

journal homepage: www.elsevier.com/locate/marpolbul

Evaluation of morphological and physiological effects of pile driving noise on marine microalgae using flow cytometry and pulse-amplitude modulated fluorometry☆

Yujung Byeon [a], Junghyun Lee [b,*], Beomgi Kim [a], Seongjin Hong [c], Jong Seong Khim [a,d,**]

[a] School of Earth and Environmental Sciences & Research Institute of Oceanography, Seoul National University, Seoul 08826, Republic of Korea
[b] Department of Environmental Education & Global AI Convergence Laboratory, Kongju National University, Gongju 32588, Republic of Korea
[c] Department of Marine Environmental Sciences, Chungnam National University, Daejeon 34134, Republic of Korea
[d] Center for Convergence Coastal Research, Seoul National University, Siheung-si, Gyeonggi-do 15011, Republic of Korea

ARTICLE INFO

Keywords:
Anthropogenic noise
Underwater noise
Offshore wind farm
Microalgae bioassay
Primary producers
Cell viability assays

ABSTRACT

Pile driving noise has emerged as a major anthropogenic stressor in marine ecosystems, yet its effects on microalgae remain largely unexplored. This study investigated the morphological and physiological responses of three marine microalgae species (*Isochrysis galbana*, *Dunaliella tertiolecta*, and *Phaeodactylum tricornutum*) to simulated pile driving noise. The analysis included assessments of growth inhibition, changes in cell size, granularity, esterase activity, membrane permeability, and photosynthetic activity, using flow cytometry and pulse-amplitude modulated fluorometry. All species exhibited significant reductions in cell size and granularity following noise exposure, with esterase activity being the most affected endpoint. Meanwhile, *I. galbana* exhibited a selective survival strategy, while *D. tertiolecta* and *P. tricornutum* employed physiological adjustments and structural adaptation. Among the species, *P. tricornutum* showed the highest sensitivity and slowest recovery to noise exposure. These findings emphasize the importance of multiple indicators beyond cell density for evaluating noise-induced stress in microalgae and provide insights into the ecological impact of underwater noise pollution on primary producers.

1. Introduction

The marine soundscape comprises a wide range of sounds originating from abiotic sources, biological processes, and anthropogenic activities (Duarte et al., 2021). Pile driving, one of the most intense anthropogenic noise sources, occurs during the construction of fixed structures such as offshore wind farms. With the increasing global demand for renewable energy, offshore wind farm construction has expanded rapidly, leading to a rise in pile driving noise in marine environments (Global Wind Energy Council, 2023). This noise is characterized by repeated, impulsive, low-frequency sounds (<1 kHz) that can propagate over long distances, potentially affecting a wide range of marine organisms (van der Knaap et al., 2022).

Marine organisms rely on natural acoustic signals for communication, predator detection, locomotion, and reproductive behavior (Slabbekoorn and Bouton, 2008; Slabbekoorn et al., 2010). Anthropogenic noise can disrupt or distort these critical functions, leading to behavioral alterations, physiological stress, and in severe cases, injury or mortality, particularly in marine mammals, fish, and invertebrates (Duarte et al., 2021). For instance, Kim et al. (2024) demonstrated that exposure to recorded pile driving noise in a controlled indoor mesocosm system negatively affected the behavior of various fish species. As such, most research on the biological effects of pile driving noise has focused primarily on larger organisms, leaving a significant gap in understanding its impact on smaller, non-hearing organisms such as microalgae.

Microalgae, despite their fundamental role as primary producers in marine ecosystems (Nestler et al., 2012), have received limited attention

☆ This article is part of a Special issue entitled: 'YES2023' published in Marine Pollution Bulletin.

* Corresponding author.
** Corresponding author at: School of Earth and Environmental Sciences & Research Institute of Oceanography, Seoul National University, Seoul 08826, Republic of Korea.
E-mail addresses: leejunghyun@kongju.ac.kr (J. Lee), jskocean@snu.ac.kr (J.S. Khim).

https://doi.org/10.1016/j.marpolbul.2025.118226
Received 1 February 2025; Received in revised form 27 April 2025; Accepted 24 May 2025
Available online 28 May 2025

regarding their responses to underwater noise. Few studies have reported that exposure to pile driving noise can reduce microalgal concentration in biofilms (Cervello et al., 2023) and decrease biomass at specific noise frequencies within the pile driving noise range (Keramati et al., 2021). Recent evidence suggests that non-hearing organisms, including microalgae, may respond not only to sound pressure but also to other components of underwater sound, including particle motion and vibration (Popper and Hawkins, 2018; Frongia et al., 2020; Cervello et al., 2023).

Microalgae are highly sensitive to various environmental stressors (Bauer et al., 2012). Underwater sound can act as a mechanical stressor, exerting physical forces such as shear stress, changes in cell membrane tension, and hydrostatic pressure. These forces may disrupt normal cellular functions (Frongia et al., 2020; Wang and Lan, 2018). Excessive shear stress, in particular, can lead to decreased cell viability, impaired photosynthetic activity, reduced growth rates, and even cell lysis (Wang and Lan, 2018; Rodríguez et al., 2009). For example, exposure to ultrasound frequencies above 20 kHz has been reported to cause physiological changes, including alterations in membrane permeability and cell rupture (Liu et al., 2022). However, existing research on the effects of pile driving noise on microalgae has primarily focused on biomass changes, with little attention given to physiological and/or morphological responses. To address this gap, this study evaluates the physiological and morphological effects of pile driving noise on microalgae by analyzing multiple biological endpoints through flow cytometry (FCM) and pulse-amplitude modulation (PAM) fluorometry.

The specific objectives of this study were to (1) evaluate the effects of pile driving noise on the growth of three microalgal species (*Isochrysis galbana*, *Dunaliella tertiolecta*, and *Phaeodactylum tricornutum*); (2) investigate its effects on morphological properties (cell size and granularity) and cell viability parameters (esterase activity and membrane permeability); (3) examine its influence on photosynthetic activity in microalgae; and (4) compare species-specific effects across various endpoints based on the characteristics of microalgae. This study provides a comprehensive evaluation of microalgal stress responses to pile driving noise exposure and offers fundamental data for assessing the biological impact of underwater noise on marine life.

2. Materials and methods

2.1. Experimental design

To assess the effects of pile driving noise on microalgae, we developed an indoor mesocosm system (80 × 110 × 30 cm) constructed with 1 cm-thick acrylic walls (Fig. 1A). An underwater speaker (UW-30, 100–10,000 Hz frequency response; University Sound, Columbus, OH, USA) was suspended at mid-depth on one end of the tank using a cord. This setup was designed to minimize internal sound reflections and prevent structure-borne vibrations by avoiding direct contact between the speaker and the tank wall (Crovo et al., 2022; Nichols et al., 2015). Additionally, acoustic panels were attached to all internal tank walls to further reduce sound reverberation within the tank (Olivier et al., 2023). The tank was filled with enough fresh water to fully submerge the speaker (water depth: 26 cm) and was maintained at 23 ± 1 °C. Fresh

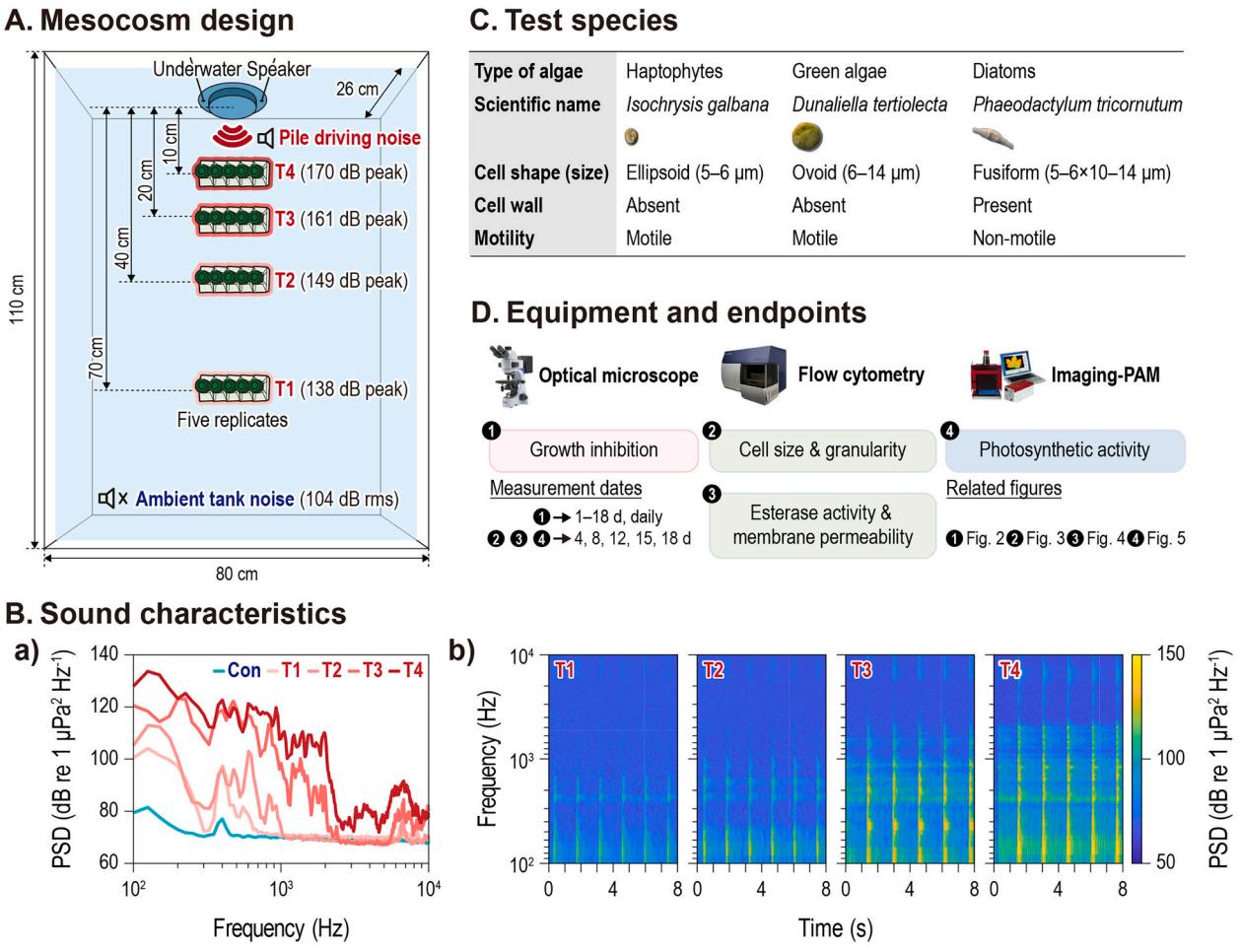

Fig. 1. (A) Mesocosm design. (B) Sound characteristics: (a) power spectral densities (PSD) and (b) spectrograms of ambient tank noise (Con) and pile driving noise (T1–T4) emitted in our experimental conditions. (C) Test species (*I. galbana*, *D. tertiolecta*, and *P. tricornutum*). (D) Equipment and endpoints used in this study.

water was used to prevent salt accumulation on equipment surfaces and to facilitate experimental manipulation. Preliminary experiments further confirmed that variations in salinity within the tank did not significantly influence the acoustic exposure conditions or experimental outcomes. This is because the microalgae were isolated within culture flasks, thereby minimizing direct interaction with the surrounding tank environment. Underwater photosynthetically active radiation (PAR) was set at 38 μmol·m^{-2}·s^{-1} using LED lighting, following a 12 h/12 h light-dark cycle. PAR was measured at the depth of the microalgal flasks using an LI-192 underwater quantum sensor connected to an LI-1500 data logger (LI-COR, Lincoln, NE, USA).

Microalgae in culture flasks were positioned at four fixed distances from the speaker (10, 20, 70, and 80 cm), with five replicates arranged horizontally at each distance. The control group was kept in the same tank as the treatment group when no playback occurred. The background noise level in the tank where the control flasks were placed was approximately 104 dB re 1 μPa (rms), comparable to typical ambient noise levels in natural marine environments (Nedwell et al., 2003). During noise playback periods, the control group was transferred to an acoustically isolated tank, while all other conditions remained consistent.

Pile driving noise was played for 3 h per day (9:00 AM–12:00 PM). The time of noise exposure was set to reflect the typical time required to install a single monopile in a real marine environment (1.5–4.5 h) (van der Knaap et al., 2022). While indoor mesocosm systems have limitations in fully replicating natural environments, they provide advantages such as controlled experimental conditions, high repeatability, and detailed observations (Kim et al., 2024).

2.2. Sound characteristics

The pile driving noise used in this study was originally recorded during the construction of the North Hoyle Offshore Wind Farm at a water depth of 5 m and a distance of 750 m from the piling site (Nedwell et al., 2003). The recording was subsequently processed into a continuous 3-h playback track using Audacity version 3.0.2 (Audacity Team; https://www.audacityteam.org). Detailed sound characteristics of the playback track are provided in Table S1 and Fig. 1B. The track was played back using an underwater speaker connected to an amplifier (CA-160, 60 W, 100–10,000 Hz, TOA Electronics, Kobe, Japan), powered by a 12 V car battery and controlled via a laptop.

Ambient noise and pile driving noise were recorded by placing a hydrophone (TC4013, 1–170,000 Hz frequency range, − 211 ± 3 dB re 1 V μPa^{-1} receiving sensitivity; Teledyne RESON, Slangerup, Denmark) inside the flask, positioned in the same configuration as the experimental conditions. The hydrophone was connected to a preamplifier (EC6081 mk2; Teledyne RESON) and a data acquisition module (NI-9234; National Instruments), following standard procedures for underwater noise measurement (Merchant et al., 2015). The recordings were band-pass filtered between 100 and 10,000 Hz. This range was selected based on the technical specifications of the playback system and the potential contamination by low-frequency noise (< 100 Hz), such as electrical noise generated by power current (Akamatsu et al., 2002). Moreover, previous studies have demonstrated that microalgae can exhibit measurable physiological responses to sound within this frequency range (Jiang et al., 2012; Keramati et al., 2021; Cai et al., 2016), supporting the biological relevance of the selected band.

The SPL of ambient and pile driving noise were calculated as root mean square (SPL_{rms}) and zero-to-peak (SPL_{z-p}) values over 10-s recording periods using hydrophone signal analysis software (HD-300; Rectuson, Changwon, South Korea). The average SPL_{rms} of ambient noise in the flasks was 104 dB re 1 μPa, while the average SPL_{z-p} values for pile driving noise treatments (T1–T4) were 138, 149, 161, and 170 dB re 1 μPa, respectively.

To further characterize the spectral properties of the noise exposure, the power spectral density (PSD) analysis was conducted using the PAM Guide acoustic package in MATLAB (R2020b; MathWorks, Natick, MA, USA) (Merchant et al., 2015). The PSD was calculated across a 100–10,000 Hz frequency range using Hann windows with 50 % overlap and 0.1-s segment lengths (Fig. 1B). As shown in Fig. 1B, the underwater noise reproduced in the tank generally reflected the typical spectral characteristics of pile driving noise, with most of its energy concentrated below 2000 Hz (Reinhall and Dahl, 2011; Nedwell et al., 2003).

2.3. Microalgal cultivation and noise exposure

We tested three species of marine microalgae representing different taxonomic groups: *Isochrysis galbana* (Haptophyta), *Dunaliella tertiolecta* (Green algae), and *Phaeodactylum tricornutum* (Diatoms) (Fig. 1C), as described in Park et al. (2024). *D. tertiolecta* and *P. tricornutum* were obtained from the UTEX Culture Collection (University of Texas, Austin, TX, USA), and *I. galbana* was provided by the Korea Marine Microalgae Culture Center (KMCC, KIOST, Geoje, Korea).

All experiments were conducted in 50 mL culture flasks with a working volume of 20 mL, using five replicates per treatment (Table S2). Microalgae were cultured according to DIN EN ISO (International Organization for Standardization) 10253 (2018), with minor modifications. The initial cell density was adjusted by diluting microalgal suspensions cultured in f/2 medium (*I. galbana*: 9×10^4 cells mL^{-1}; *D. tertiolecta*: 5×10^4 cells mL^{-1}; *P. tricornutum*: 7×10^4cells mL^{-1}). While the ISO 10253-2016 recommends an initial cell density below 10^4 cells mL^{-1}, this study aimed to evaluate multiple endpoints, including cell viability and photosynthetic activity, in addition to assessing growth inhibition. To obtain reliable and reproducible data, a minimum cell density above 10^5 cells mL^{-1} and an initial fluorescence (F_o) > 0.075 were required for FCM and PAM fluorometry, respectively (Čertnerová and Galbraith, 2021; Stock et al., 2019). Accordingly, the minimum initial cell density for each species was determined based on their growth rates to ensure a sufficient number of cells for each analysis (Lee et al., 2023; An et al., 2021; Ivošević DeNardis et al., 2023).

After 72 h of exposure, the growth rate of the control group was significantly lower than that suggested by the standard protocol (ISO 10253, 2016). This was most likely due to reduced light penetration due to the experimental setup, in which the microalgal culture flasks with lids were submerged in a water tank. Using an open beaker-type vessel for noise exposure would have allowed better light penetration. However, culture flasks were specifically chosen to prevent contamination, ensure uniform noise exposure among replicates at the same distance, and eliminate potential noise reduction effects caused by the container itself. Thus, based on the observed growth rates of microalgae, the noise exposure period was set to 12 days to allow the evaluation of its effects during the exponential growth phase. After the noise exposure period, the culture flasks were moved out of the tank to minimize light limitation while maintaining all other conditions constant. Observations then continued for six days to determine whether the cells had reached a steady state. Cell counting was performed daily, while flow cytometry and PAM fluorescence analysis, which require a sufficient number of cells for reliable measurements, were conducted starting on day 4 and subsequently on days 8, 12, 15, and 18 (Fig. 1D).

2.4. Assessment of growth inhibition

The cell number in replicate samples was estimated using an Olympus CKX53 microscope (Olympus Corporation, Tokyo, Japan) and a disposable hemocytometer (InCyto, South Korea). The resulting measurements were used to calculate the intrinsic growth rate (μ) and growth inhibition ($I_{\mu i}$). The intrinsic growth rate (μ) was calculated using Eq. 1, where N_0 represents the initial cell density and N_t is the cell density after t hours. The growth inhibition ($I_{\mu i}$) was calculated according to Eq. 2, where μ_i is the growth rate of the culture flask i and μ_C is the average growth rate of the control group (ISO10253, 2016).

$$\mu = \frac{\mathrm{In}\,(N_t) - \mathrm{In}(N_0)}{t} \quad (1)$$

$$I_{\mu i}(\%) = \frac{\mu_c - \mu_i}{\mu_c} \times 100 \quad (2)$$

2.5. Flow cytometry analysis

Flow cytometry analysis was performed using a BD FACS Canto II flow cytometer (BD Biosciences, San Jose, USA) equipped with three lasers (405, 488, and 633 nm) and eight filters. For each sample, 10,000 cells were measured; if this number was not reached, samples were analyzed for 1 min. The staining method and conditions for each endpoint were adapted from Lee et al. (2015) with some modifications (Table S3). Data were analyzed using FlowJo V10 software (FlowJo LLC, Ashland, OR, USA).

The endpoints measured through FCM analysis represent microalgal inherent properties and cell viability. Forward scatter (FSC) reflects cell size, while side scatter (SSC) represents cell granularity. *I. galbana* and *D. tertiolecta* were dual-stained with fluorescein diacetate (FDA) for esterase activity and SYTOX Blue for membrane permeability to assess cell viability under noise exposure conditions (Lee et al., 2020). This dual-staining method allows for the simultaneous measurement and interpretation of multiple cell characteristics. The distribution of dot plots (Q1–Q4) resulting from dual-staining is described in Fig. S1. In contrast, propidium iodide (PI) staining was more effective for assessing the membrane permeability of *P. tricornutum*. However, PI staining may cause potential emission overlap with FDA. To avoid this, single staining was exclusively applied to *P. tricornutum* (Fig. S1) (Olsen et al., 2016).

2.6. PAM fluorometry analysis

PAM fluorometry (IMAGING-PAM, Heinz Walz GmbH, Effeltrich, Germany) in conjunction with the ImagingWin software (Heinz Walz GmbH PAM, Effeltrich, Germany) was employed to assess the photosynthetic activity of microalgae exposed to pile driving noise, following the method described by Almeida et al. (2019). On days 4, 8, 12, 15, and 18, 1 mL of each *I. galbana*, *D. tertiolecta,* and *P. tricornutum* culture was centrifuged at 4200 rpm for 20 min at room temperature. After centrifugation, 800 μL of the supernatant was removed, and the remaining 200 μL containing the pellet was transferred to a 96-well plate (Corning Incorporated, Costar®, NY, USA). Additionally, measurements were performed at the same time each day under the same settings (measuring light intensity, frequency, and gain) across all species.

Seven parameters were measured, including the effective PS II quantum yield (*Y(II)*), quantum yield of regulated energy dissipation (*Y(NPQ)*), quantum yield of non-regulated energy dissipation (*Y(NO)*), coefficient of photochemical quenching (*qP* and *qL*), coefficient of non-photochemical quenching (*qN*), and electron transport rate (*ETR*). All endpoints assessed through Imaging-PAM analysis were calculated using the formulas presented in Table S4.

2.7. Statistics analysis

The normality of the data was assessed using the Shapiro–Wilk test prior to subsequent analyses. To evaluate the effects of pile driving noise on microalgal growth inhibition, cell size, granularity, esterase activity, membrane permeability, and maximum electron transport rate (rETR$_{max}$), a one-way analysis of variance (ANOVA), followed by Tukey's HSD post hoc test, was conducted to compare group differences. If the data did not meet the normality assumptions, a Kruskal–Wallis test was applied as a non-parametric alternative. All statistical analyses were performed using SPSS 25.0 (IBM Corporation, Chicago, IL, USA). A p-value <0.05 was considered statistically significant.

To assess the correlation between the SPL of pile driving noise and the measured endpoints, Pearson's correlation analysis was performed in RStudio (Posit PBC, Boston, MA, USA), and the results were visualized using the 'corrplot' package in R (Wei et al., 2017). Principal component analysis (PCA) was conducted to interpret and visually represent the microalgal endpoint results using PRIMER v6 (PRIMER-E Ltd., Plymouth, UK). Missing values were imputed using the mean of the corresponding group.

3. Results and discussion

3.1. Growth inhibition of microalgae under noise exposure

During the 12-day noise exposure period, the average growth rates of the control group ranged from 0.3 to 0.4 day^{-1}, indicating that the experimental setup adequately supported normal microalgal growth (Borg-Stoveland et al., 2024). Among the tested species, *I. galbana* exhibited the highest cell density during this period (Fig. 2). This is likely due to its smaller cell size compared to the other two species, as smaller cells are generally associated with faster growth rates (Agusti and Kalff, 1989; Schlesinger et al., 1981) (Fig. 1C).

On the final day of noise exposure (day 12), *I. galbana* showed minimal growth inhibition (0.1–0.5 %) under T1–T3 (138–161 dB re 1 μPa) conditions. However, significant growth inhibition (7.5 %) was observed at the highest noise level (T4, 170 dB re 1 μPa) ($p < 0.05$). In contrast, *D. tertiolecta* and *P. tricornutum* exhibited substantial growth inhibition (~11 %) even at the lowest noise level (T1, 138 dB re 1 μPa) (both $p < 0.05$). Notably, *D. tertiolecta* showed a gradual increase in growth inhibition, reaching 16.0 % under T4 ($p < 0.05$).

The playback noise generated in the experiment exhibited high energy within the low-frequency range (100–2000 Hz) (Fig. 1B), which could have affected microalgal growth. Microalgae detect and respond to specific sound frequencies via mechanosensitive ion channels in their cell membranes, regulating cellular activities such as ion flow and signal transduction (Frongia et al., 2020). Therefore, prolonged exposure to noise at specific frequencies can interrupt signal transduction pathways, impair metabolic functions, and ultimately lead to reduced cell growth (Frongia et al., 2020; Tambunan et al., 2020). Moreover, increasing sound intensity at a given frequency can amplify physical effects such as pressure fluctuations, particle motion, and vibration (Campbell et al., 2019), thereby intensifying the mechanical impact on cells. These findings are consistent with previous studies reporting growth inhibition in *Dunaliella salina* exposed to 1000 Hz sound waves (Keramati et al., 2021; Cervello et al., 2023).

Although mesocosm-based experiments provide a controlled environment to assess biological responses to acoustic stimuli, it is acknowledged that such conditions may not fully replicate the natural marine soundscapes. In particular, particle motion and vibration can be highly localized near the speaker or tank boundaries, and these components were not quantified in the present study, which may limit the interpretation of the observed responses (Popper and Hawkins, 2016). While efforts were made to minimize structural vibrations and acoustic reflections by suspending the speaker and installing acoustic panels, minor mechanical disturbances or electromagnetic influences associated with the experimental setup could not be entirely ruled out. These potential confounding factors may have partially affected the physiological responses observed in microalgae and should be carefully considered in the design and interpretation of future experiments.

Species-specific differences sensitivity to pile driving noise may be influenced by both cell size and structural features, such as the presence or absence of a cell wall (Fig. 1C). *P. tricornutum* possesses a silicified cell wall that provides structural stability, whereas *D. tertiolecta* and *I. galbana* are enclosed only by a plasma membrane, potentially rendering them more vulnerable to mechanical stress (Oren, 2005; Liu and Lin, 2000; Le Costaouëc et al., 2017). Additionally, larger cells have a greater surface area exposed to micro-eddies, making them more prone to structural damage (Hadiyanto et al., 2013). Considering these factors, the higher growth inhibition observed in *D. tertiolecta* can be partially

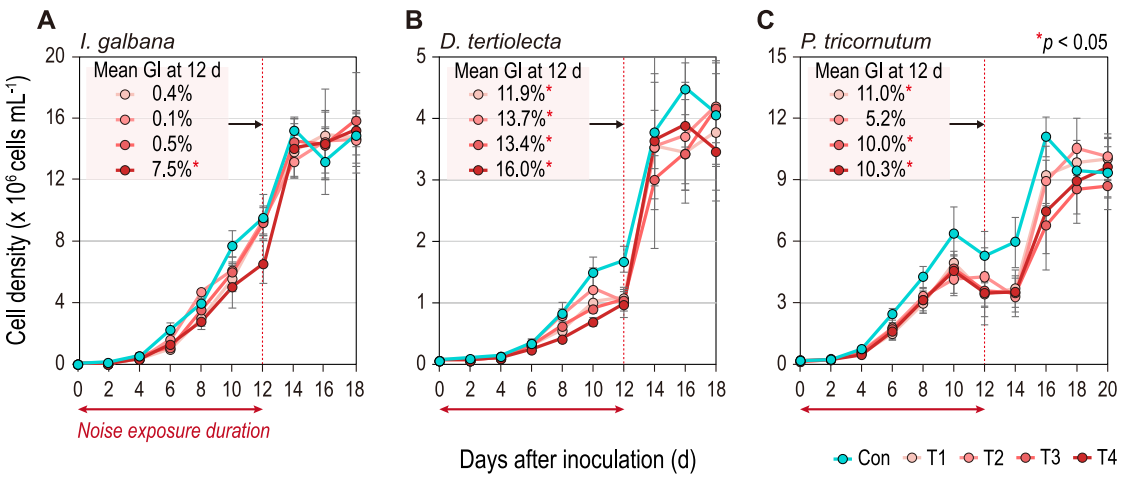

Fig. 2. Cell density of three microalgal species over 18 (or 20) days under ambient tank noise (Con) and pile driving noise (T1–T4). Growth inhibition (GI) on day 12 is expressed numerically. Data are presented as mean ± standard deviation ($N = 5$). The asterisk (*) indicates a significant difference ($\boldsymbol{p < 0.05}$) compared to the control group.

attributed to its lack of a cell wall and its relatively larger cell size compared to *I. galbana*.

Following the noise exposure period (days 12–18), all experimental groups showed an accelerated increase in cell density, likely due to the relocation of culture flasks. However, this increase did not indicate a return to the exponential growth phase. Rather, cells transitioned into the senescence phase, cell density stabilized, and the gap between the control and experimental groups gradually narrowed. To assess whether the differences in growth rate during the exponential phase resulted from morphological and physiological responses to noise exposure, we conducted further analyses.

3.2. Morphological responses of microalgae under noise exposure

Following noise exposure, the mean SSC (cell size) values of all treatment groups were significantly lower than those of the control group ($p < 0.05$) by day 8, and the mean FSC (cell granularity) values also exhibited a general decreasing trend compared to the control (Fig. 3). These results suggested that underwater noise exposure induced morphological changes in the microalgae (Fig. 3). Among the three tested species, *P. tricornutum* exhibited the greatest reductions, with both mean FSC and SSC values decreasing by approximately 0.8-fold (20 %) relative to the control. *P. tricornutum* possesses a facultatively silicified cell wall that allows high morphological plasticity, enabling transitions among fusiform, oval, and triradiate forms. Under

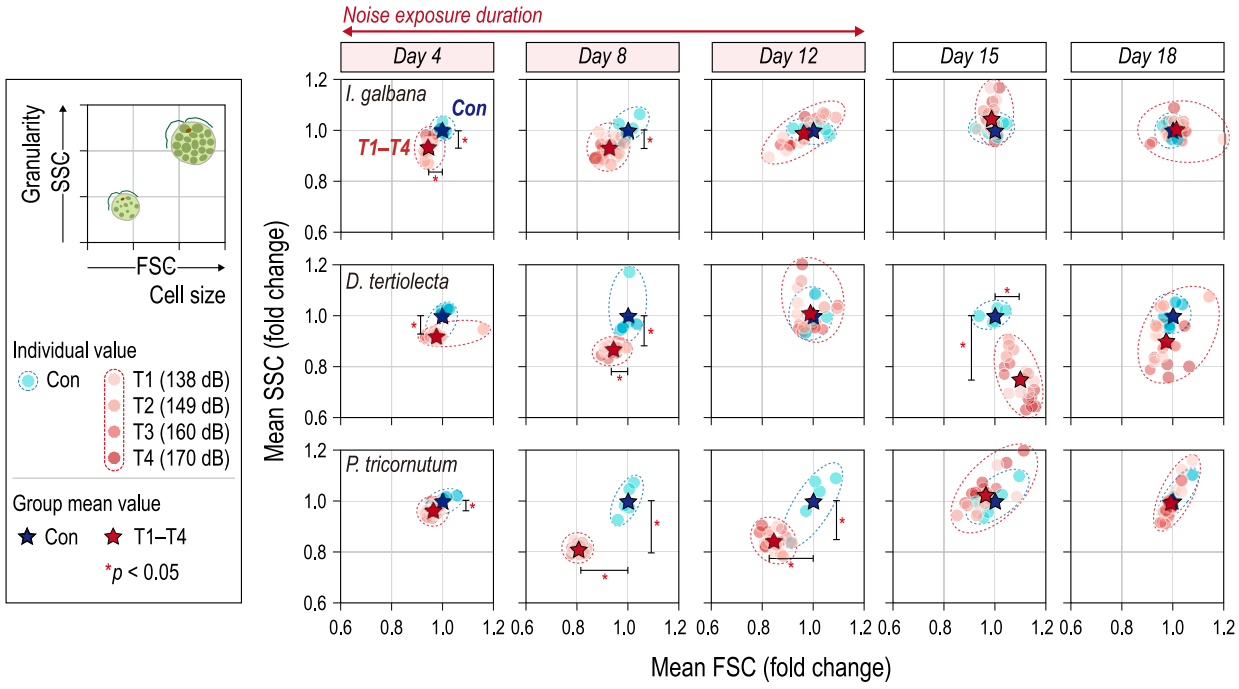

Fig. 3. Changes in forward scatter (FSC, cell size) and side scatter (SSC, granularity) signals in the three species under ambient tank noise (Con) and pile driving noise (T1–T4). The mean values of approximately 10,000 cell particles per replicate ($N = 5$) are represented by transparent dots, with dashed lines indicating the range of the control and treatment groups. The overall mean values for the control and treatment groups are shown as blue and red stars, respectively. The asterisk (*) indicates a significant difference ($\boldsymbol{p < 0.05}$) compared to the control group. (For interpretation of the references to colour in this figure legend, the reader is referred to the web version of this article.)

environmental stress, transitions toward the oval form have been reported to initiate within approximately 3–5 days, with a notable increase in oval cells observed between days 8 and 12 (De Martino et al., 2011). Oval cells are characterized by smaller cell size compared to fusiform or triradiate forms, thicker silica-based cell walls, accumulation of lipid bodies, and disorganization of chloroplast structures (De Martino et al., 2011; Borowitzka and Volcani, 1978). Therefore, the observed decreases in FSC and SSC in this study can be attributed to such stress-induced morphological transitions.

Notably, the reductions in FSC and SSC values for *P. tricornutum* persisted through day 12 consistent with the delayed growth pattern described in Section 3.1. These species-specific differences likely reflect the intrinsic biological characteristics of *P. tricornutum*, such as its extended cell cycle, investment in facultative silicification, and adoption of conservative stress responses under unfavorable conditions (Matsumura et al., 2003). In *I. galbana* and *D. tertiolecta*, cell size and cell granularity no longer showed significant differences from the control group by day 12. Simultaneously, the alleviation of light limitation following the relocation of culture flasks facilitated a rapid increase in cell densities. In contrast, *P. tricornutum* reached its maximum cell density only by day 16, further reflecting its delayed division associated with stress adaptation mechanisms (Matsumura et al., 2003).

Interestingly, on day 15, *D. tertiolecta* in the treatment groups had a mean SSC value that was 0.8-fold lower and a mean FSC value that was 1.1-fold higher than in the control group (both $p < 0.05$) (Table S5). This pattern suggests that cell swelling may have been induced by stress. The fact that this phenomenon was observed only in *D. tertiolecta* is likely attributable to its thin, flexible, and cellulose-deficient cell membrane, making it more susceptible to morphological alterations (Oren, 2005). Prolonged cell swelling can expand the cell membrane beyond its structural limits, leading to irreversible damage or complete cell lysis (Liu et al., 2022).

3.3. Physiological responses of microalgae under noise exposure

The fluorescence analysis using FCM revealed two distinct patterns in the noise-exposed treatment groups (Fig. 4). The first pattern (Pattern 1) was characterized by the emergence of two separate fluorescence peaks: one similar to the control group and another exhibiting a significant shift in fluorescence intensity. In contrast, the second pattern (Pattern 2) exhibited a single peak that slightly overlapped with the control but showed a uniform shift in fluorescence intensity across the entire cell population. Pattern 1 reflects the phenomenon in which individual cell fluorescence signals split into two distinct groups, whereas Pattern 2 represents a gradual shift in the overall population. Considering these differences, Pattern 1 was evaluated by analyzing the proportion of cells corresponding to the second peak, while Pattern 2 was quantified using the mean fluorescence intensity (MFI) value (Fig. 4A). *I. galbana* exhibited Pattern 1, while *D. tertiolecta* and *P. tricornutum* followed Pattern 2.

Patterns of esterase activity and membrane permeability varied in timing and magnitude among the three species. *I. galbana* exhibited an increase in both esterase inactivation and membrane permeability on day 15, whereas *D. tertiolecta* and *P. tricornutum* showed only increased esterase inactivation on days 12 and 8, respectively, without major changes in membrane permeability (Fig. 4A; Table S6). In detail, on day 15, under the highest pile driving noise level (T4, 170 dB re 1 μPa), *I. galbana* exhibited a simultaneous decrease in esterase activity and increased membrane permeability (Fig. 4B). Consequently, 16.9 % of the total cell population localized in the Q4 region, indicative of severe cellular damage (Hammes et al., 2011). Moreover, the cells displayed a dichotomous distribution predominantly between Q1 (healthy cells) and Q4 (cells undergoing apoptosis or necrosis), rather than occupying intermediate regions such as Q2 or Q3. This distinct pattern explains the formation of two peaks observed in Pattern 1. These findings are consistent with the growth inhibition results (Fig. 2), suggesting that although the cell numbers increased after day 12, the cells transitioned into the senescence phase rather than resuming exponential growth.

For *D. tertiolecta*, approximately 98 % of the control group cells were located in Q1, but as the SPL_{z-p} of pile driving noise increased, a gradual shift toward Q3 was observed. By T4, the proportion of cells in Q3 increased to 62.1 %, surpassing the Q1 population (36.7 %). Similarly, *P. tricornutum* showed a decrease in FDA fluorescence in the treatment groups compared to the control, whereas no significant changes were observed in PI fluorescence, which represents membrane permeability. This suggests that the cell wall of *P. tricornutum* provides structural stability, preventing membrane damage, while *D. tertiolecta*, with its flexible cell membrane, undergoes morphological changes but does not experience significant membrane damage (Oren, 2005). As a result, *D. tertiolecta* exhibited reduced physiological activity and cell swelling under noise exposure, but did not reach the stage of complete cell death.

These interspecies differences can be interpreted as variations in survival strategies. *I. galbana* appears to adopt a selective survival strategy, where a portion of the population undergoes severe damage and apoptosis, while the remaining cells maintain viability by preserving esterase activity and membrane integrity. This suggests that *I. galbana* may utilize programmed cell death (PCD) or stress-induced apoptosis mechanisms as an adaptive response (Affenzeller et al., 2009; Gallo et al., 2017). Considering its small cell size and rapid growth rate, *I. galbana* likely achieves greater energy efficiency by eliminating damaged cells and promoting rapid division rather than investing energy in the maintenance or repair of compromised cells. In contrast, *D. tertiolecta* and *P. tricornutum* regulate metabolic rates rather than undergoing immediate cell death, effectively optimizing energy utilization under stress conditions (Behrenfeld et al., 2008). This strategy allows them to minimize unnecessary energy expenditure and maintain cellular integrity in response to noise exposure (Behrenfeld et al., 2008). These species-specific survival strategies align with findings from previous studies investigating microalgal responses to suspended sediments and polycyclic aromatic hydrocarbons (An et al., 2021, 2023; Park et al., 2024). The consistency of response patterns across different types of stressors suggests that the survival strategies observed in microalgae are likely robust and stable, regardless of the specific nature of the environmental disturbance. These distinct physiological responses may influence not only individual survival but also population-level dynamics in natural marine ecosystems. For instance, selective survival and rapid turnover in *I. galbana* could allow for faster recovery following transient stress events, potentially conferring a competitive advantage in fluctuating environments. Meanwhile, the stress tolerance strategies of *D. tertiolecta* and *P. tricornutum* may enable persistence under prolonged or repeated stress, thereby contributing to community resilience. Although a variety of environmental stressors are likely to exert stronger pressures in the field, noise-induced physiological modulation, as demonstrated in this study, could act as an additional factor influencing species succession and phytoplankton assemblage structure in anthropogenically disturbed waters (Wang et al., 2024).

Under natural environmental conditions, microalgal responses are influenced by the combined effects of multiple, co-occurring stressors. For example, offshore wind farm construction introduces micro-environmental stressors such as wake effects, shading, increased suspended sediments, and nutrient fluctuations, all of which can alter primary production and ecosystem dynamics (Daewel et al., 2021; Kordan and Yakan, 2024). Within this complex framework, noise-induced physiological responses, as demonstrated in this study, noise-induced stress may act synergistically with other anthropogenic disturbances, further reshaping phytoplankton community structure and ecosystem functioning.

3.4. Photosynthetic responses of microalgae under noise exposure

Each microalgal species exhibited distinct rapid light curves (RLCs), with varying rETR values and light saturation points (Jesus et al., 2023).

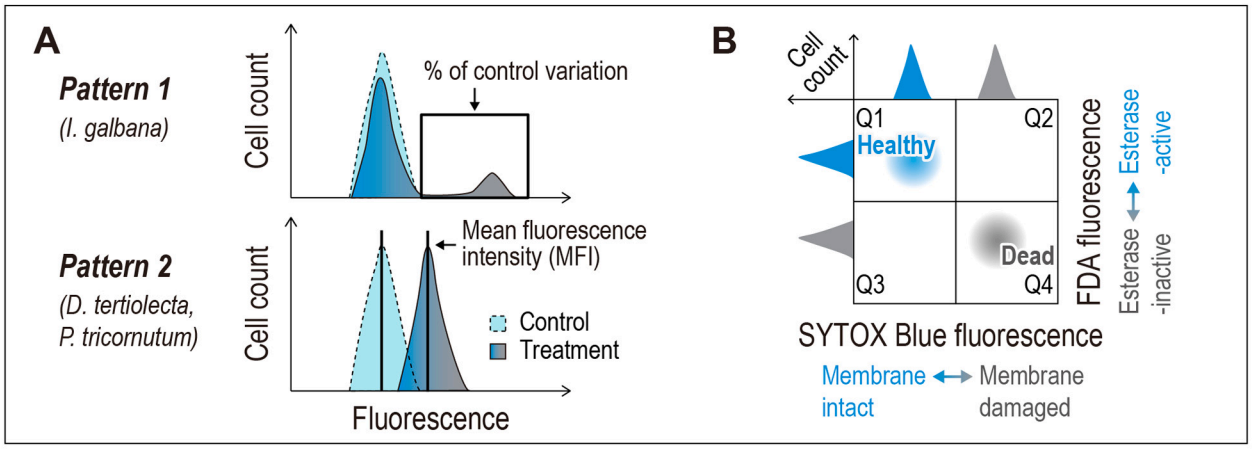

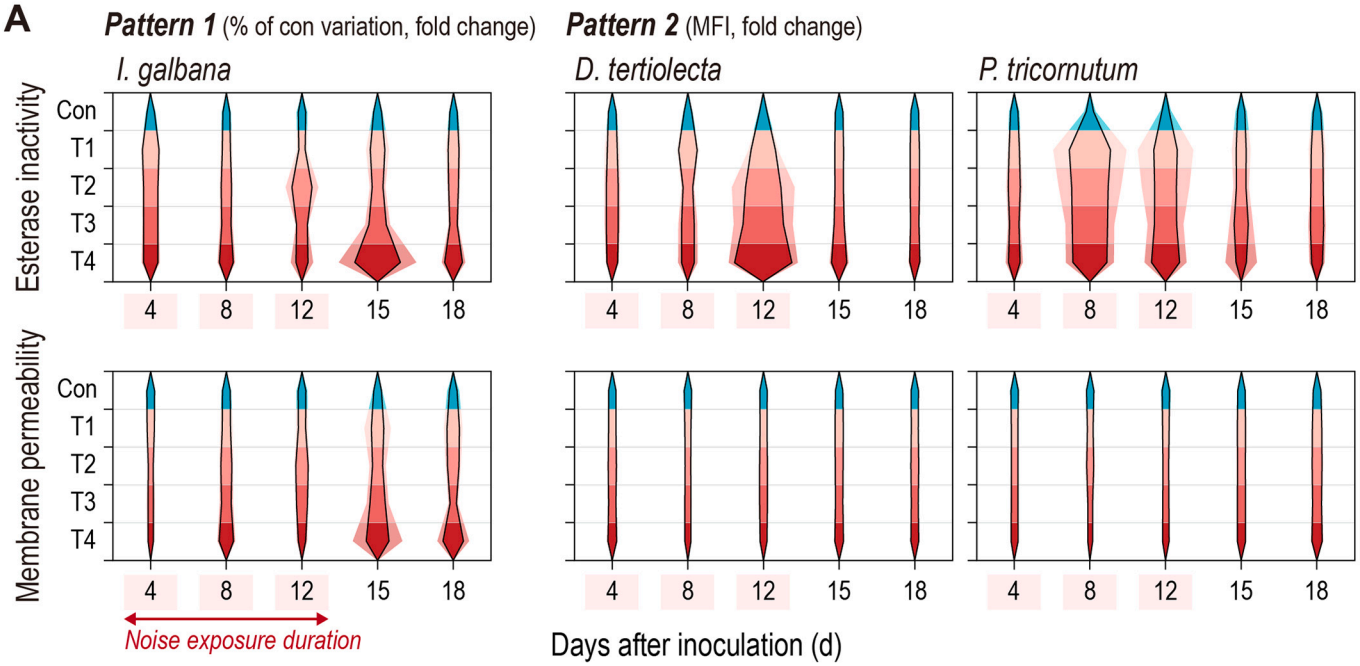

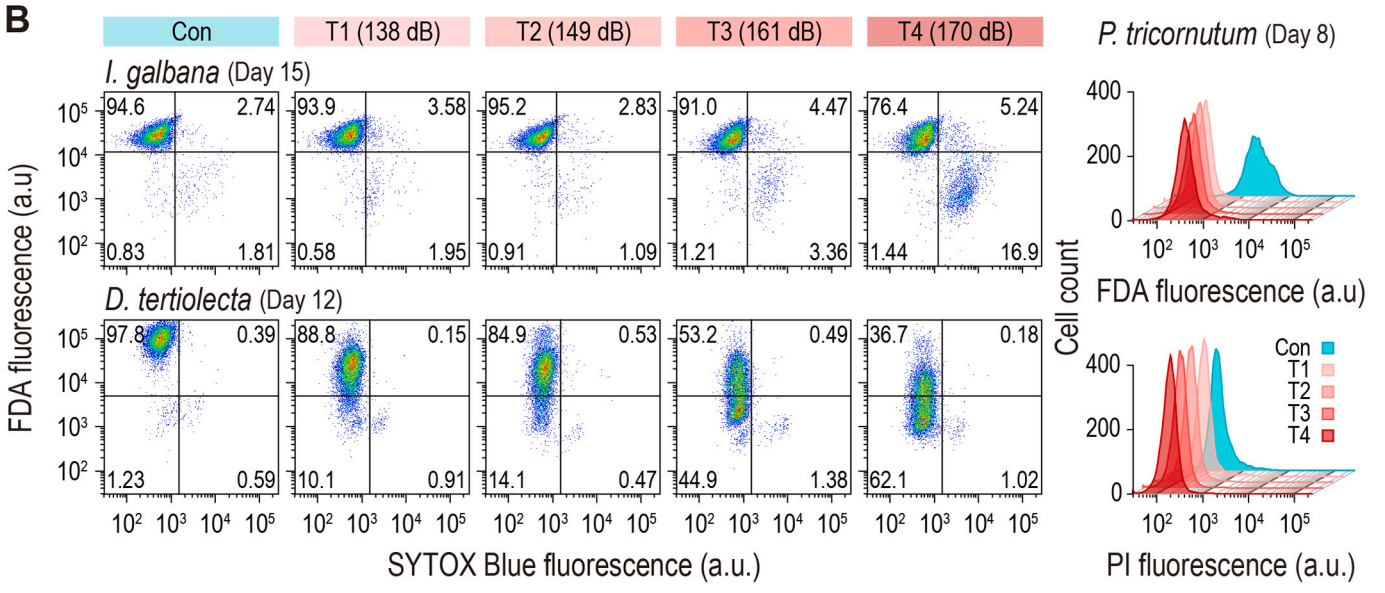

(caption on next page)

Fig. 4. Species-specific changes in FDA (esterase activity) and SYTOX or PI fluorescence (membrane permeability) under pile driving noise exposure. Cells were classified in a four-quadrant plot based on FDA fluorescence and SYTOX Blue fluorescence. In *P. tricornutum*, PI was used instead of SYTOX Blue, and the results are presented as histograms. (A) Results for *I. galbana* are expressed as the percentage of control variation for FDA and SYTOX Blue fluorescence. For *D. tertiolecta* and *P. tricornutum,* results are represented as mean fluorescence intensity (MFI) of FDA and SYTOX Blue or PI. Since FDA fluorescence is inversely proportional to esterase activity, MFI^{-1} values were used for FDA fluorescence. All values are expressed as fold changes relative to the control group. (B) Flow cytometry dot plots for *I. galbana* (day 15) and *D. tertiolecta* (day 12) with FDA and SYTOX Blue and histograms for *P. tricornutum* (day 8) with FDA and PI. Each dot represents one cell particle and colors denote relative particle density in each population. (For interpretation of the references to colour in this figure legend, the reader is referred to the web version of this article.)

A comparison of the mean $rETR_{max}$ values between the control and T4 revealed a reduction of 4.5 in *I. galbana* on day 4 of noise exposure (Fig. 5). The decrease in $rETR_{max}$ indicates a decline in the photochemical efficiency of photosystem II, suggesting an overall negative impact on photosynthesis-related responses (Ralph and Gademann, 2005). This reduction is consistent with phenomena commonly observed under stress conditions such as chemical pollution, nutrient limitation, and high temperatures (Figueroa et al., 2019; Abbew et al., 2022; White et al., 2011). *D. tertiolecta* and *P. tricornutum* exhibited weak or undectable fluorescence signals, likely due to low cell density and insufficient chlorophyll *a* (Sjollema et al., 2014).

On day 8 of noise exposure, *I. galbana* still exhibited a reduction in $rETR_{max}$ between the control and T4 group, but the magnitude of this decrease was reduced to 2.2, compared to day 4. The decline in rETR followed a trend similar to the growth inhibition observed in the treatment groups (Fig. 2), which aligns with previous studies reporting a correlation between rETR values and growth rate (Wang et al., 2023a). On day 12, this pattern was reversed, with the mean $rETR_{max}$ of the treatment groups exceeding that of the control, particularly in the T4, where the mean $rETR_{max}$ difference between the control and T4 was significantly higher by approximately 4.7 ($p < 0.05$). This reversal is likely attributed to early depletion of nutrients such as nitrogen and phosphorus in the control group, where higher growth rates led to faster nutrient consumption (Fig. 2). Previous studies have also shown that as nutrients in the culture medium become depleted, chlorophyll and other photosynthetic pigments are synthesized at lower rates, leading to reduced light absorption and consequently a decrease in rETR (Figueroa et al., 2014; Cheng et al., 2019; Wang et al., 2023b).

Meanwhile, *D. tertiolecta* exhibited a sharp decline in rETR in the T4group at 287 μmol photons m^{-2} s^{-1} (PAR) on day 8, but the mean $rETR_{max}$ values showed no significant difference from the control group until day 12. A reversal in mean $rETR_{max}$ was observed on day 15, when the highest cell density was reached, although the magnitude of the reversal was not as pronounced as that observed in *I. galbana* on day 12. These results suggest that *D. tertiolecta* employs a survival strategy that involves regulating its overall metabolic rate to optimize energy use.

P. tricornutum exhibited a significant reduction in mean $rETR_{max}$ under pile driving noise conditions of 161 dB re 1 μPa (T3) or higher, with significant differences observed in both treatments ($p < 0.05$), on day 8. These decreases coincided with the period when cell size and granularity showed the greatest reduction, suggesting a strong link between morphological changes and photosynthetic efficiency. As previously discussed, this phenomenon may be attributed to the species-specific characteristics of *P. tricornutum*, which involves a morphological transition to the oval form under environmental stress. In these stressed cells, the disorganization of chloroplast thylakoid membranes has been reported, leading to suppressed photosynthetic activity and a likely metabolic shift from active growth to a survival mode (Borowitzka and Volcani, 1978; De Martino et al., 2011; Flori et al., 2017).

Notably, unlike the other two species, *P. tricornutum* did not exhibit a reversal in $rETR_{max}$ within the treatment groups, although the difference between the control and treatment groups gradually diminished until convergence. This finding suggests that *P. tricornutum* may have a relatively low capacity to recover from noise-induced stress, potentially due to either persistent damage to the photosynthetic machinery or the delayed recovery of metabolic activity. These physiological limitations are consistent with the delayed cell division and growth suppression previously observed in *P. tricornutum* following noise exposure.

3.5. Relationship between pile driving noise and endpoints

To further investigate the relationship between pile driving noise and

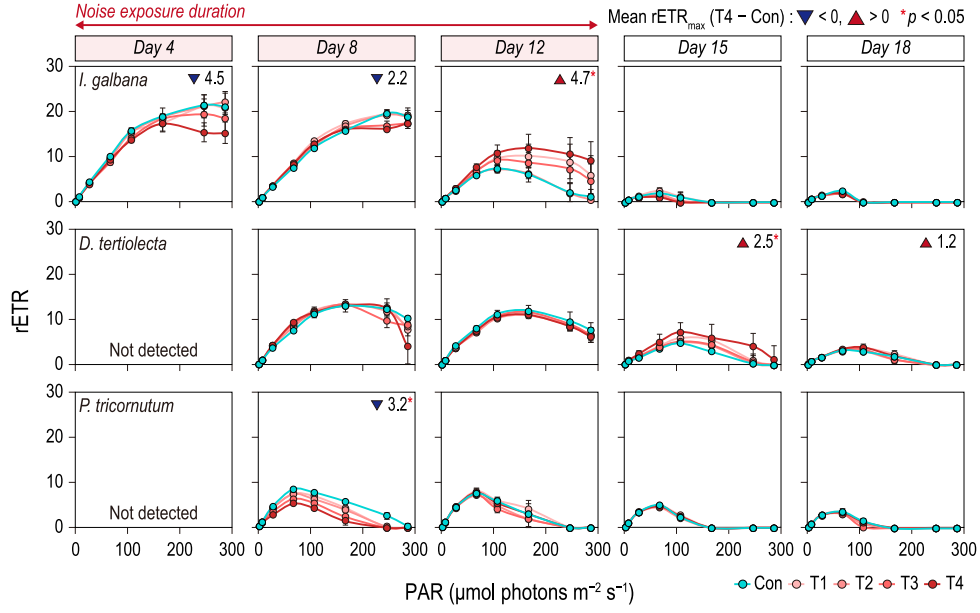

Fig. 5. Rapid light curves for *I. galbana*, *D. tertiolecta,* and *P. tricornutum* days under ambient tank noise (Con) and pile driving noise (T1–T4). Data are presented as mean ± standard deviation ($N = 5$).

microalgal responses, correlation analysis and PCA were conducted (Fig. 6; Table S7). Pearson's correlation analysis revealed a general negative correlation between $SPL_{z\text{-}p}$ of pile driving noise and cell density across all measurement days, indicating that an increase in pile driving noise led to a decrease in cell density (Fig. 6A). In particular, *D. tertiolecta* and *P. tricornutum* exhibited significant negative correlations, whereas *I. galbana* did not show a significant correlation. This suggests that the rapid division rate and selective survival strategy of *I. galbana* allow it to maintain cell numbers well under noise exposure. After noise exposure ended, cell density increased in *I. galbana* and *D. tertiolecta*, whereas *P. tricornutum* continued to show a negative correlation, suggesting that *P. tricornutum* has a relatively lower recovery capacity from noise-induced stress.

A negative correlation between $SPL_{z\text{-}p}$ of pile driving noise and esterase activity was observed in all species and at all measurement points, but the magnitude and timing of the response varied among species. In *I. galbana*, a significant negative correlation was observed on day 4 ($r = -0.61$, $p < 0.05$), while in *D. tertiolecta*, the correlation became significant on day 12 ($r = -0.75$, $p < 0.05$). The rapid increase in *D. tertiolecta* cell numbers between days 12 and 14 may explain this pattern, as dividing cells tend to be larger with weaker cell walls, making them more vulnerable to shear stress (Michels et al., 2016; Camacho et al., 2007).

Membrane permeability, which is generally considered an indicator of cell damage, did not show a consistent trend. This may be because membrane permeability is influenced not only by cellular damage but also by an increased proportion of newly generated young cells with underdeveloped membranes (Yan et al., 2021). As a result, measuring esterase activity may provide a more effective indicator of physiological stress caused by noise exposure than membrane permeability.

Among the three species, *P. tricornutum* exhibited the highest number of significant correlations between $SPL_{z\text{-}p}$ of pile driving noise and various endpoints, indicating greater sensitivity to noise exposure. Interestingly, the conversion of *P. tricornutum* to the oval form, characterized by a thicker cell wall, may mitigate internal damage, as no significant correlation was observed between noise exposure and esterase activity. This suggests that evaluating cell size and granularity may be more appropriate for assessing *P. tricornutum*'s response to noise exposure than esterase activity.

PCA results showed distinct grouping patterns among species in response to noise exposure (Fig. 6). Chl-*a*, measured via FCM, and $rETR_{max}$, measured using PAM fluorometry, were positioned closely together in the PCA plot, indicating their interdependence in determining photosynthetic efficiency. This supports previous findings that higher Chl-*a* content enhances light absorption, leading to increased rETR. In *I. galbana*, Y(II) (effective PSII quantum yield) was closely aligned with ETR and Chl-*a*, suggesting a strong correlation among these key photosynthetic variables. Thus, Chl-*a* content in *I. galbana*, measured via FCM, may serve as an indirect indicator of photosynthetic activity.

I. galbana maintained higher photosynthetic activity despite noise exposure, likely due to its selective survival strategy, which ensures that surviving cells continue to function efficiently. These findings suggest that evaluating only growth inhibition may not fully capture the impact of pile driving noise on microalgae, and incorporating physiological indicators provides a more comprehensive assessment. Conversely, *D. tertiolecta* and *P. tricornutum* more effectively reflected the impact of noise exposure through cell density changes. In addition, Y(NO) (quantum yield of non-regulated energy dissipation) increased with higher noise levels, indicating that non-regulated energy dissipation played a more significant role in these species under noise exposure. Since Y(NO) is associated with PSII damage under stress conditions, this

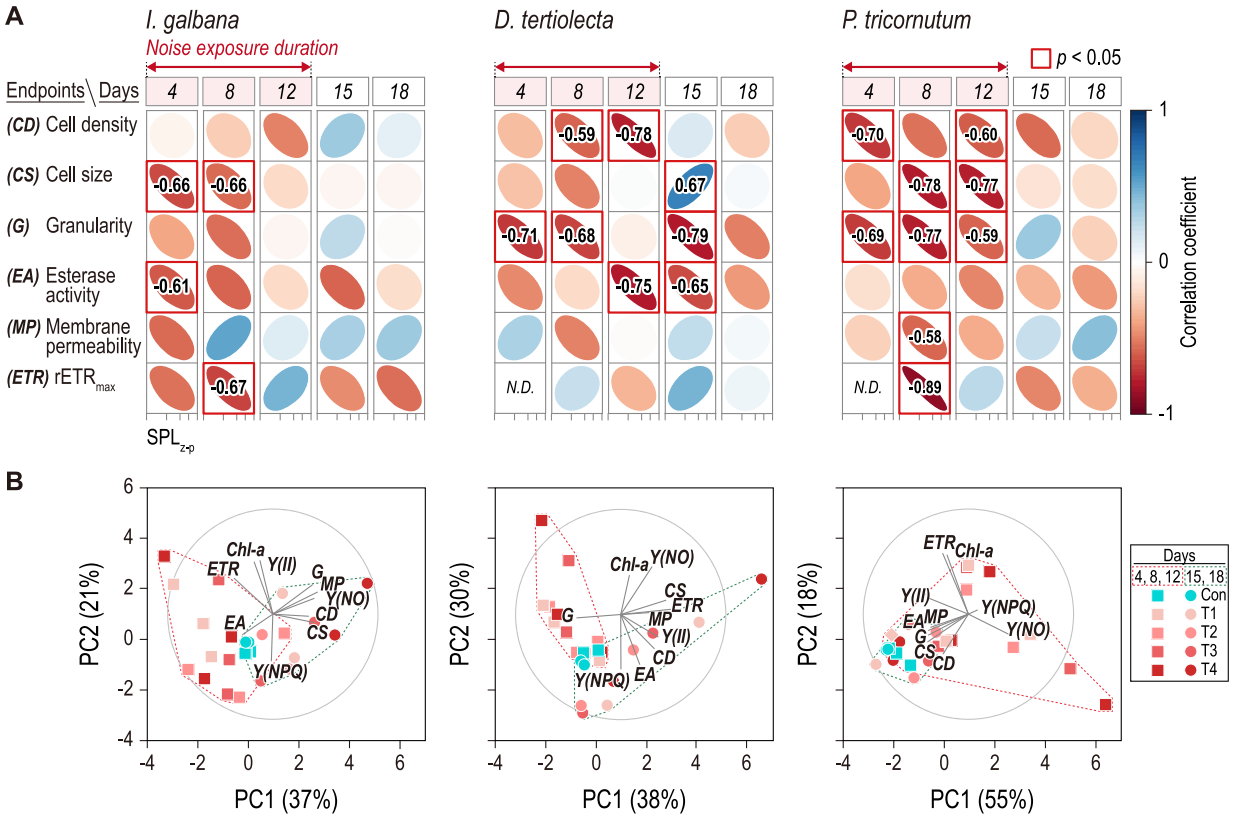

Fig. 6. (A) Pearson's correlation coefficient (r) between sound pressure $level_{z\text{-}p}$ of pile driving noise (Con: 117 dB; T1: 138 dB; T2: 149 dB; T3: 161 dB; T4: 170 dB) and responses of each endpoints. (B) Principal Component Analysis (PCA) results for the three species under pile driving noise treatments (Con, T1–T4). Some variables are abbreviated as follows: CD = cell density, CS = cell size, G = granularity, EA = esterase activity, MP = membrane permeability, Chl-*a* = chlorophyll-*a*, ETR = maximal electron transfer rate.

finding suggests that pile driving noise may have increased PSII photodamage in *D. tertiolecta* and *P. tricornutum*. The observed changes in various physiological indicators and species-specific traits suggest that noise exposure could exert complex impacts on marine ecosystem functioning. Reductions in cell size, cytoplasmic complexity, and photosynthetic efficiency may lead to declines in primary production, while differences in species-specific recovery rates could alter community composition, thereby weakening functional diversity and ecosystem stability. Moreover, stress-induced morphological transitions, such as increased prevalence of oval forms, may reduce the efficiency of energy flow and nutrient cycling, ultimately impacting higher trophic levels and disrupting food web dynamics. These cascading effects could, in the long term, diminish the resilience of marine ecosystems to environmental disturbances.

4. Conclusions

This study emphasizes the species-specific morphological and physiological responses of marine microalgae to pile driving noise, revealing distinct survival strategies and adaptive responses. While *I. galbana* maintained esterase activity, membrane integrity, and photosynthetic efficiency in most surviving cells through a selective survival strategy, *D. tertiolecta,* and *P. tricornutum* exhibited suppressed physiological activity, potentially reflecting an adaptive approach to limit energy expenditure and sustain survival under stress conditions. These interspecies differences are closely associated with inherent biological traits, including cell size, growth rate, cell wall structure, and morphological plasticity. Notably, *P. tricornutum* displayed greater sensitivity and delayed recovery following noise exposure, suggesting that certain taxa may experience more pronounced and long-lasting impacts from underwater noise pollution. Moreover, the observed correlations between noise exposure, esterase activity, and photosynthetic activity highlight the importance of physiological indicators in assessing noise-induced stress beyond conventional growth inhibition. These findings highlight that microalgal responses to anthropogenic noise could have cascading ecological consequences, emphasizing the need for more comprehensive biological assessments. Future research should focus on long-term adaptation mechanisms, as well as the broader ecological implications of noise-induced stress on marine microbial community structure and function.

CRediT authorship contribution statement

Yujung Byeon: Writing – original draft, Visualization, Formal analysis, Data curation, Conceptualization. **Junghyun Lee:** Writing – review & editing, Writing – original draft, Visualization, Supervision, Methodology, Data curation. **Beomgi Kim:** Data curation, Methodology. **Seongjin Hong:** Formal analysis, Data curation. **Jong Seong Khim:** Writing – review & editing, Supervision, Project administration, Methodology, Conceptualization.

Declaration of competing interest

The authors declare that they have no known competing financial interests or personal relationships that could have appeared to influence the work reported in this paper.

Acknowledgments

This research was supported by Korea Institute of Marine Science & Technology Promotion (KIMST) funded by the Ministry of Oceans and Fisheries (RS-2021-KS211469 and RS-2024-00417889). This work was also supported by National Research Foundation of Korea (NRF) grants funded by the Korean government (RS-2025-00521903).

Appendix A. Supplementary data

Supplementary data to this article can be found online at https://doi.org/10.1016/j.marpolbul.2025.118226.

Data availability

Data will be made available on request.

References

Abbew, A.W., Qiu, S., Amadu, A.A., Qasim, M.Z., Chen, Z., Wu, Z., Ge, S., 2022. Insights into the multi-targeted effects of free nitrous acid on the microalgae *Chlorella sorokiniana* in wastewater. Bioresour. Technol. 347, 126389. https://doi.org/10.1016/j.biortech.2021.126389.

Affenzeller, M.J., Darehshouri, A., Andosch, A., Lütz, C., Lütz-Meindl, U., 2009. Salt stress-induced cell death in the unicellular green alga *Micrasterias denticulata*. J. Exp. Bot. 60 (3), 939–954. https://doi.org/10.1093/jxb/ern334.

Agusti, S., Kalff, J., 1989. The influence of growth conditions on the size dependence of maximal algal density and biomass. Limnol. Oceanogr. 34 (6), 1104–1108. https://doi.org/10.4319/lo.1989.34.6.1104.

Akamatsu, T., Okumura, T., Novarini, N., Yan, H.Y., 2002. Empirical refinements applicable to the recording of fish sounds in small tanks. J. Acoust. Soc. Am. 112 (6), 3073–3083. https://doi.org/10.1121/1.1515799.

Almeida, A.C., Gomes, T., Habuda-Stani'c, M., Lomba, J., Romi'c, Z., Turkalj, J.V., Lillicrap, A., 2019. Characterization of multiple biomarker responses using flow cytometry to improve environmental hazard assessment with the green microalgae *Raphidocelis subcapitata*. Sci. Total Environ. 687, 827–838. https://doi.org/10.1016/j.scitotenv.2019.06.009.

An, S.A., Lee, J., Cha, J., Gwak, J., Kim, M., Hur, J., Hong, S., Khim, J.S., 2023. Characterization of microalgal toxicants in the sediments from an industrial area: application of advanced effect-directed analysis with multiple endpoint bioassays. Environ. Int. 173, 107833. https://doi.org/10.1016/j.envint.2023.107833.

An, S.-A., Hong, S., Lee, J., Cha, J., Lee, S., Moon, H.B., Giesy, J.P., Khim, J.S., 2021. Identification of potential toxicants in sediments from an industrialized area in Pohang, South Korea: application of a cell viability assay of microalgae using flow cytometry. J. Hazard. Mater. 405, 124230. https://doi.org/10.1016/j.jhazmat.2020.124230.

Bauer, D.E., Conforti, V., Ruiz, L., Gómez, N., 2012. An in situ test to explore the responses of *Scenedesmus acutus* and *Lepocinclis acus* as indicators of the changes in water quality in lowland streams. Ecotoxicol. Environ. Saf. 77, 71–78. https://doi.org/10.1016/j.ecoenv.2011.11.019.

Behrenfeld, M.J., Halsey, K.H., Milligan, A.J., 2008. Evolved physiological responses of phytoplankton to their integrated growth environment. Philos. Trans. R. Soc. B Biol. Sci. 363 (1504), 2687–2703. https://doi.org/10.1098/rstb.2008.0019.

Borg-Stoveland, S., Draganovic, V., Spilling, K., Gabrielsen, T.M., 2024. Successful growth of coastal marine microalgae in wastewater from a salmon recirculating aquaculture system. J. Appl. Phycol. 1–11. https://doi.org/10.1007/s10811-024-03310-1.

Borowitzka, M.A., Volcani, B.E., 1978. The polymorphic diatom *Phaeodactylum tricornutum*: ultrastructure of its morphotypes. J. Phycol. 14 (1), 10–21. https://doi.org/10.1111/j.1529-8817.1978.tb00625.x.

Cai, W., Dunford, N.T., Wang, N., Zhu, S., He, H., 2016. Audible sound treatment of the microalgae *Picochlorum oklahomensis* for enhancing biomass productivity. Bioresour. Technol. 202, 226–230. https://doi.org/10.1016/j.biortech.2015.12.012.

Camacho, F.G., Gallardo Rodríguez, J.J., Sánchez Mirón, A., Cerón García, M.C., Belarbi, E.H., Molina Grima, E., 2007. Determination of shear stress thresholds in toxic dinoflagellates cultured in shaken flasks. Process Biochem. 42, 1506–1515. https://doi.org/10.1016/j.procbio.2007.07.011.

Campbell, J., Sabet, S.S., Slabbekoorn, H., 2019. Particle motion and sound pressure in fish tanks: a behavioural exploration of acoustic sensitivity in the zebrafish. Behav. Process. 164, 38–47. https://doi.org/10.1016/j.beproc.2019.04.003.

Čertnerová, D., Galbraith, D.W., 2021. Best practices in the flow cytometry of microalgae. Cytometry A 99 (4), 359–364. https://doi.org/10.1002/cyto.a.24278.

Cervello, G., Olivier, F., Chauvaud, L., Winkler, G., Mathias, D., Juanes, F., Tremblay, R., 2023. Impact of anthropogenic sounds (pile driving, drilling and vessels) on the development of model species involved in marine biofouling. Front. Mar. Sci. 10, 1111505. https://doi.org/10.3389/fmars.2023.1111505.

Cheng, J., Wang, Z., Lu, H., Xu, J., He, Y., Cen, K., 2019. Hydrogen sulfide promotes cell division and photosynthesis of *Nannochloropsis oceanica* with 15% carbon dioxide. ACS Sustain. Chem. Eng. 7 (19), 16344–16354. https://doi.org/10.1021/acssuschemeng.9b03293.

Crovo, J.A., Mendonça, M.T., Johnston, C.E., 2022. Acoustic modulation of reproductive hormones in the blacktail shiner, *Cyprinella venusta*, a soniferous cyprinid. Anim. Behav. 186, 101–106. https://doi.org/10.1016/j.anbehav.2022.01.008.

Daewel, U., Akhtar, N., Christiansen, N., Schrum, C., 2021. Offshore wind farms are projected to impact primary production and bottom water deoxygenation in the North Sea. Commun. Earth Environ. 3, 292. https://doi.org/10.1038/s43247-022-00625-0.

De Martino, A., Bartual, A., Willis, A., Meichenin, A., Villazán, B., Maheswari, U., Bowler, C., 2011. Physiological and molecular evidence that environmental changes elicit morphological interconversion in the model diatom *Phaeodactylum tricornutum*. Protist 162 (3), 462–481. https://doi.org/10.1016/j.protis.2011.02.002.

DIN EN ISO (International Organization for Standardization) 10253, 2018. Water quality-marine algal growth inhibition test with *Skeletonema* sp. and *Phaeodactylum tricornutum*. International Organization for Standardization, Switzerland. https://doi.org/10.1007/s10811-023-03105-w.

Duarte, C.M., Chapuis, L., Collin, S.P., Costa, D.P., Devassy, R.P., Eguiluz, V.M., Erbe, C., Gordon, T.A.C., Halpern, B.S., Harding, H.R., Havlik, M.N., Meekan, M., Merchant, N.D., Miksis-Olds, J.L., Parsons, M., Predragovic, M., Radford, A.N., Radford, C.A., Simpson, S.D., Slabbekoorn, H., Staaterman, E., Van Opzeeland, I.C., Winderen, J., Zhang, X., Juanes, F., 2021. The soundscape of the Anthropocene ocean. Science 371, 1–10. https://doi.org/10.1126/science.aba4658.

Figueroa, F.L., Domínguez-González, B., Korbee, N., 2014. Vulnerability and acclimation to increased UVB radiation in three intertidal macroalgae of different morpho-functional groups. Mar. Environ. Res. 97, 30–38. https://doi.org/10.1016/j.marenvres.2014.02.004.

Figueroa, F.L., Celis-Plá, P.S., Martínez, B., Korbee, N., Trilla, A., Arenas, F., 2019. Yield losses and electron transport rate as indicators of thermal stress in *Fucus serratus* (Ochrophyta). Algal Res. 41, 101560. https://doi.org/10.1016/j.algal.2019.101560.

Flori, S., Jouneau, P.-H., Bailleul, B., Gallet, B., Estrozi, L.F., Moriscot, C., Bastien, O., Eicke, S., Schober, A., Río Bártulos, C., et al., 2017. Plastid thylakoid architecture optimizes photosynthesis in diatoms. Nat. Commun. 8, 15885. https://doi.org/10.1038/ncomms15885.

Frongia, F., Forti, L., Arru, L., 2020. Sound perception and its effects in plants and algae. Plant Signal. Behav. 15 (12), 1828674. https://doi.org/10.1080/15592324.2020.1828674.

Gallo, C., d'Ippolito, G., Nuzzo, G., Sardo, A., Fontana, A., 2017. Autoinhibitory sterol sulfates mediate programmed cell death in a bloom-forming marine diatom. Nat. Commun. 8 (1), 1292. https://doi.org/10.1038/s41467-017-01435-5.

Global Wind Energy Council, 2023. Global offshore wind report 2023. https://gwec.net/global-offshore-wind-report-2023/.

Hadiyanto, H., Elmore, S., Van Gerven, T., Stankiewicz, A., 2013. Hydrodynamic evaluations in high rate algae pond (HRAP) design. Chem. Eng. J. 217, 231–239. https://doi.org/10.1016/j.cej.2012.12.081.

Hammes, F., Berney, M., Egli, T., 2011. Cultivation-independent assessment of bacterial viability. High Resolut. Microb. Single Cell Anal. 123–150. https://doi.org/10.1007/978-94-007-3840-1_9.

ISO10253, 2016. Water quality-marine algal growth inhibition test with *Skeletonema costatum* and *Phaeodactylum tricornutum*. International Organization for Standardization, Switzerland.

Ivošević DeNardis, N., Novosel Vlašić, N., Mišić Radić, T., Zemła, J., Lekka, M., Demir-Yilmaz, I., Formosa-Dague, C., Levak Zorinc, M., Vrana, I., Juraić, K., Horvat, L., Žutinić, P., Gligora Udovič, M., Gašparović, B., 2023. Behavior and surface properties of microalgae indicate environmental changes. J. Appl. Phycol. 36 (1), 113–128. https://doi.org/10.1007/s10811-023-03105-w.

Jesus, B., Jauffrais, T., Trampe, E., Méléder, V., Ribeiro, L., Bernhard, J.M., Geslin, E., Kühl, M., 2023. Microscale imaging sheds light on species-specific strategies for photo-regulation and photo-acclimation of microphytobenthic diatoms. Environ. Microbiol. 25 (12), 3087–3103. https://doi.org/10.1111/1462-2920.16499.

Jiang, S., Rao, H., Chen, Z., Liang, M., Li, L., 2012. Effects of sonic waves at different frequencies on propagation of *Chlorella pyrenoidosa*. J. Agric. Sci. 4 (6), 68–75. https://doi.org/10.5539/jas.v4n6p68.

Keramati, A., Shariati, F.P., Tavakoli, O., Akbari, Z., Rezaei, M., 2021. The effect of audible sound frequency on the growth and beta-carotene production of *Dunaliella salina*. S. Afr. J. Bot. 141, 373–382. https://doi.org/10.1016/j.sajb.2021.05.012.

Kim, B., Jin, G., Byeon, Y., Park, S.Y., Lee, C., Lee, J., Khim, J.S., 2024. Pile driving noise impacts behavioral patterns of important east Asian juvenile marine fishes. Mar. Pollut. Bull. 207, 116893. https://doi.org/10.1016/j.marpolbul.2023.116893.

van der Knaap, I., Slabbekoorn, H., Moens, T., Van den Eynde, D., Reubens, J., 2022. Effects of pile driving sound on local movement of free-ranging Atlantic cod in the Belgian North Sea. Environ. Pollut. 300, 118913. https://doi.org/10.1016/j.envpol.2022.118913.

Kordan, M.B., Yakan, S.D., 2024. The effect of offshore wind farms on the variation of the phytoplankton population. Reg. Stud. Mar. Sci. 69, 103358. https://doi.org/10.1016/j.rsma.2023.103358.

Le Costaouëc, T., Unamunzaga, C., Mantecon, L., Helbert, W., 2017. New structural insights into the cell-wall polysaccharide of the diatom *Phaeodactylum tricornutum*. Algal Res. 26, 172–179. https://doi.org/10.1016/j.algal.2017.07.023.

Lee, J., Choi, E.J., Rhie, K., 2015. Validation of algal viability treated with total residual oxidant and organic matter by flow cytometry. Mar. Pollut. Bull. 97 (1–2), 95–104. https://doi.org/10.1016/j.marpolbul.2015.06.024.

Lee, J., Hong, S., Kim, T., Lee, C., An, S.-A., Kwon, B.-O., Lee, S., Moon, H.-B., Giesy, J.P., Khim, J.S., 2020. Multiple bioassays and targeted and nontargeted analyses to characterize potential toxicological effects associated with sediments of Masan Bay: focusing on AhR-mediated potency. Environ. Sci. Technol. 54, 4443–4454. https://doi.org/10.1021/acs.est.9b06995.

Lee, J., Hong, S., An, S.-A., Khim, J.S., 2023. Methodological advances and future directions of microalgal bioassays for evaluation of potential toxicity in environmental samples: a review. Environ. Int. 173, 107869. https://doi.org/10.1016/j.envint.2023.107869.

Liu, C.-P., Lin, L.-P., 2000. Ultrastructural study and lipid formation of *Isochrysis* sp. CCMP1324. Bot. Bull. Acad. Sin. 42, 207–214.

Liu, Y., Liu, X., Cui, Y., Yuan, W., 2022. Ultrasound for microalgal cell disruption and product extraction: a review. Ultrason. Sonochem. 87, 106054. https://doi.org/10.1016/j.ultsonch.2022.106054.

Matsumura, K., Yagi, T., Yasuda, K., 2003. Role of timer and sizer in regulation of *Chlamydomonas* cell cycle. Biochem. Biophys. Res. Commun. 306 (4), 1042–1049. https://doi.org/10.1016/S0006-291X(03)01061-9.

Merchant, N.D., Fristrup, K.M., Johnson, M.P., Tyack, P.L., Witt, M.J., Blondel, P., Parks, S.E., 2015. Measuring acoustic habitats. Methods Ecol. Evol. 6 (3), 257–265. https://doi.org/10.1111/2041-210X.12330.

Michels, M.H.A., van der Goot, A.J., Vermuë, M.H., Wijffels, R.H., 2016. Cultivation of shear stress sensitive and tolerant microalgal species in a tubular photobioreactor equipped with a centrifugal pump. J. Appl. Phycol. 28, 53–62. https://doi.org/10.1007/s10811-015-0563-2.

Nedwell, J., Langworthy, J., Howell, D., 2003. Assessment of sub-sea acoustic noise and vibration from offshore wind turbines and its impact on marine wildlife; initial measurements of underwater noise during construction of offshore windfarms, and comparison with background noise. In: Subacoustech report ref: 544R0424 published by COWRIE.

Nestler, H., Groh, K.J., Schönenberger, R., Behra, R., Schirmer, K., Eggen, R.I., Suter, M.-J.-F., 2012. Multiple-endpoint assay provides a detailed mechanistic view of responses to herbicide exposure in *Chlamydomonas reinhardtii*. Aquat. Toxicol. 110, 214–224. https://doi.org/10.1007/s10811-023-03105-w.

Nichols, T.A., Anderson, T.W., Širović, A., 2015. Intermittent noise induces physiological stress in a coastal marine fish. PLoS One 10 (9), e0139157. https://doi.org/10.1371/journal.pone.0139157.

Olivier, F., Gigot, M., Mathias, D., Bonnel, J., Jezequel, Y., Meziane, T., et al., 2023. Impacts of anthropogenic sounds on early stages of benthic invertebrates: the 'Larvosonic system'. Limnol. Oceanogr. Methods 21, 53–68. https://doi.org/10.1002/lom3.10500.

Olsen, R.O., Hess-Erga, O.K., Larsen, A., Hoffmann, F., Thuestad, G., Hoell, I.A., 2016. Dual staining with CFDA-AM and SYTOX blue in flow cytometry analysis of UV-irradiated *Tetraselmis suecica* to evaluate vitality. Aquat. Biol. 25, 39–52. https://doi.org/10.3354/ab00656.

Oren, A., 2005. A hundred years of *Dunaliella* research: 1905–2005. Saline Syst. 1, 2. https://doi.org/10.1186/1746-1448-1-2.

Park, S.Y., Lee, J., Kwon, I., Song, H., Kim, B., Kim, T., Lee, C., Yoon, S.J., Noh, J., Hong, S., Khim, J.S., 2024. Ecotoxicological effects of suspended sediments on marine microalgae using flow cytometry and pulse-amplitude modulation (PAM) fluorometry. Mar. Pollut. Bull. 208, 116968. https://doi.org/10.1016/j.marpolbul.2024.116968.

Popper, A.N., Hawkins, A.D., 2016. The effects of noise on aquatic life II. In: Popper, A. N., Hawkins, A.D. (Eds.), The effects of noise on aquatic life II. Springer, New York, pp. 459–463. https://doi.org/10.1007/978-1-4939-2981-8_54.

Popper, A.N., Hawkins, A.D., 2018. The importance of particle motion to fishes and invertebrates. J. Acoust. Soc. Am. 143 (1), 470–488. https://doi.org/10.1121/1.5021594.

Ralph, P.J., Gademann, R., 2005. Rapid light curves: a powerful tool to assess photosynthetic activity. Aquat. Bot. 82 (3), 222–237. https://doi.org/10.1016/j.aquabot.2005.02.006.

Reinhall, P.G., Dahl, P.H., 2011. Underwater Mach wave radiation from impact pile driving: Theory and observation. J. Acoust. Soc. Am. 130 (3), 1209–1216. https://doi.org/10.1121/1.3614540.

Rodríguez, J.J., Mirón, A.S., Camacho, F.G., García, M.C., Belarbi, E.H., Chisti, Y., Grima, E.M., 2009. Causes of shear sensitivity of the toxic dinoflagellate *Protoceratium reticulatum*. Biotechnol. Prog. 25, 792–800. https://doi.org/10.1002/btpr.150.

Schlesinger, D.A., Molot, L.A., Shuter, B.J., 1981. Specific growth rates of freshwater algae in relation to cell size and light intensity. Can. J. Fish. Aquat. Sci. 38 (9), 1052–1058. https://doi.org/10.1139/f81-141.

Sjollema, S.B., van Beusekom, S.A., van der Geest, H.G., Booij, P., de Zwart, D., Vethaak, A.D., Admiraal, W., 2014. Laboratory algal bioassays using PAM fluorometry: effects of test conditions on the determination of herbicide and field sample toxicity. Environ. Toxicol. Chem. 33 (5), 1017–1022. https://doi.org/10.1002/etc.2520.

Slabbekoorn, H., Bouton, N., 2008. Soundscape orientation: a new field in need of sound investigation. Anim. Behav. 76 (4), e5–e8. https://doi.org/10.1016/j.anbehav.2008.06.010.

Slabbekoorn, H., Bouton, N., van Opzeeland, I., Coers, A., ten Cate, C., Popper, A.N., 2010. A noisy spring: the impact of globally rising underwater sound levels on fish. Trends Ecol. Evol. 25 (7), 419–427. https://doi.org/10.1016/j.tree.2010.04.005.

Stock, W., Blommaert, L., Daveloose, I., Vyverman, W., Sabbe, K., 2019. Assessing the suitability of imaging-PAM fluorometry for monitoring growth of benthic diatoms. J. Exp. Mar. Biol. Ecol. 513, 35–41. https://doi.org/10.1016/j.jembe.2018.12.003.

Tambunan, R.M.N., Santoso, Y.A., Soekirno, S., Nasruddin, N., Prihantini, N.B., 2020. Cultivation of *Chlorella* DPK-01 using audible sound (music) as a potential strategy for improving photobioreactor system. AIP Conf. Proc. 2255 (1). https://doi.org/10.1063/5.0013759.

Wang, C., Lan, C.Q., 2018. Effects of shear stress on microalgae–a review. Biotechnol. Adv. 36 (4), 986–1002. https://doi.org/10.1016/j.biotechadv.2018.02.004.

Wang, L., Wang, B., Cen, W., Xu, R., Huang, Y., Zhang, X., Han, Y., Zhang, Y., 2024. Ecological impacts of the expansion of offshore wind farms on trophic level species of marine food chain. J. Environ. Sci. 139, 226–244. https://doi.org/10.1016/j.jes.2023.05.002.

Wang, S., Zhao, Q., Yu, H., Du, X., Zhang, T., Sun, T., Song, W., 2023b. Assessing the potential of *Chlorella* sp. phycoremediation liquid digestates from brewery wastes mixture integrated with bioproduct production. Front. Bioeng. Biotechnol. 11, 1199472. https://doi.org/10.3389/fbioe.2023.1199472.

Wang, Z., Cheng, J., Guo, D., Chen, L., You, X., Tang, Y., Chen, S., Chu, F., 2023a. A novel simulation calculation model based on photosynthetic electron transfer for microalgal growth prediction in any photobioreactor. Appl. Energy 334, 120713. https://doi.org/10.1016/j.apenergy.2022.120713.

Wei, T., Simko, V., Levy, M., Xie, Y., Jin, Y., Zemla, J., 2017. Package 'corrplot'. Statistician 56 (316), e24.
White, S., Anandraj, A., Bux, F., 2011. PAM fluorometry as a tool to assess microalgal nutrient stress and monitor cellular neutral lipids. Bioresour. Technol. 102 (2), 1675–1682. https://doi.org/10.1016/j.biortech.2010.09.064.
Yan, N., Tang, B.Z., Wang, W.X., 2021. Cell cycle control of nanoplastics internalization in phytoplankton. ACS Nano 15 (7), 12237–12248. https://doi.org/10.1021/acsnano.1c01226.